Alpha-induced reactions in iridium

M. K. Bhardwaj, I. A. Rizvi, and A. K. Chaubey
Department of Physics, Aligarh Muslim University, Aligarh 202002, India
(Received 25 November 1991)

The excitation function of (α,xn) reactions on ^{191}Ir (abundance 37.3%) and on ^{193}Ir (abundance 62.7%) has been measured for the 17–55 MeV alpha-particle bombarding energy range. The stacked foil activation technique and γ-ray spectroscopy were used to determine the cross sections. The experimental data were compared with calculated values obtained by means of a geometry-dependent hybrid model. The initial exciton number $n_0=4$ with $n=2$, $p=2$, and $h=0$ gives the best agreements with the presently measured results. To calculate the excitation function theoretically a computer code was used. This set of excitation functions provides a data basis for probing the validity of combined equilibrium and preequilibrium reaction models in a considerable energy range.

PACS number(s): 25.55.−e

I. INTRODUCTION

During the last decade a lot of study has been done in understanding of nonequilibrium reaction mechanisms. The high-energy tail observed in the excitation function of the light particle reactions contains important information about the reaction mechanisms. Several models [1–8] have been proposed to interpret this experimentally observed feature of the excitation functions. The hybrid and geometry-dependent hybrid models [5,6] are found to give the best verification for the above-mentioned fact in a broad range of experimental data. More elaborate quantum-mechanical theories [9–15] which are not applied to routinely measurable preequilibrium cross sections have tended to support the foundation on which the classical models are built [16]. Presently the measurements are performed to compare the excitation function of the reactions in the isotopes of the natural iridium with Blann's geometry-dependent hybrid (GDH) model via the code ALICE, which contains both the compound and preequilibrium (PE) processes. We have measured the excitation function of the reactions ^{191}Ir(α,n), ^{191}Ir$(\alpha,2n)$, ^{191}Ir$(\alpha,3n)$, ^{191}Ir$(\alpha,4n)$, ^{191}Ir$(\alpha,5n)$, ^{193}Ir$(\alpha,3n)$, ^{193}Ir$(\alpha,4n)$, and ^{193}Ir$(\alpha,5n)$ and reported them to the best of our knowledge.

II. EXPERIMENTAL PROCEDURE

A. Sample preparation

Samples of the element under study were made from spectroscopic iridium having purity better than 99.99% by the vacuum evaporation technique in the target division of the variable Energy Cyclotron Centre, Calcutta, India. The target foils were squares of side, 1.5 cm, and of the thickness, 150 μg/cm^2. The foils were fixed on aluminium sheets having a circular hole with a diameter of 1.2 cm in its center. The aluminium degraders of the different thickness were also inserted in the target stack so that the alpha beam of 55 MeV energy might be degraded considerably.

B. Irradiation and counting

The target stack was irradiated with a 55 MeV energy alpha-particle beam at the Variable Energy Cyclotron Centre (VECC), Calcutta, India for 3900 sec, keeping in view the thickness of the sample, the melting point of the element, and the half-lives of the yields. A typical experimental setup for the stack irradiation is shown in Fig. 1. After cooling, the target foils were brought, one by one to the counting room and the residual activity was recorded with the help of a 100 cm^3 ORTEC Ge(Li) detector coupled with a precalibrated 4096 multichannel analyzer and associated electronics. The efficiency and energy calibrations were performed using a standard ^{152}Eu point source of known strength keeping it at target position.

C. Flux measurements

During the irradiation of the stack, the counting of the incoming α particles was done from an integrated beam charge. Here the beam was totally stopped in the electrically insulted irradiation heads serving as a kind of Faraday cup [17–21] where secondary electrons were prevented from escaping. Using this charge, the flux was calcu-

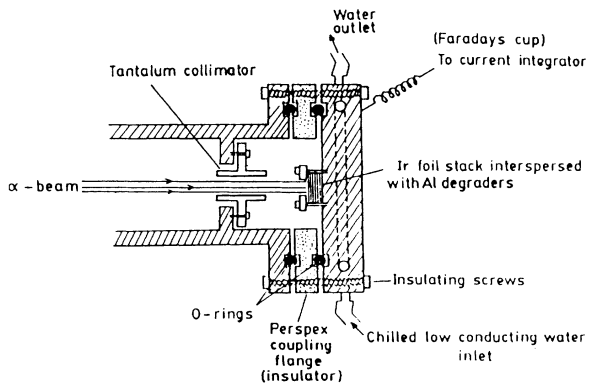

FIG. 1. Experimental setup for stack foil irradiation with an α-particle beam.

lated. Copper foil was used as a flux monitor [18] for checking the flux and good agreement was found with $< 10\%$ discrepancy.

D. Energy spread

The important factors contributing to the energy spread of the α particles incident on a particular target foil are the spread in the initial beam energy, foil thickness, stopping power values, and path length. In the present measurements, the uncertainty in the initial beam energy was ± 0.5 MeV.

The stopping power values are adopted from the tables of Northcliffe and Schilling [22], which are accurate within 5%.

Multiple scattering at small angles increases the path length of the stopping materials [23]. However, in the case of α particles, the path length correction is very small [17] ($\leq 0.5\%$) and, hence, neglected.

E. Cross-section determination

The activation cross section was computed using the following expression [19–21,24]:

$$\sigma(E)=\frac{A\lambda\exp(\lambda t_2)}{N\Phi(G\epsilon)\theta K[1-\exp(-\lambda t_1)][1-\exp(-\lambda t_3)]},$$

where A is the count under the photopeak of characteristic γ rays, λ is the decay constant of product nucleus, N is the number of nuclei of the isotope under investigation, Φ is the incident α-particle flux, $(G\epsilon)$ is the geometry-dependent efficiency of the Ge(Li) detector, θ is the absolute intensity of the characteristic γ rays, K is the self-absorption correction factor for the γ rays in the sample, t_1 is the irradiation time, t_2 is the time lapsed between stopping the beam and start of counting, and t_3 is the counting time.

The cross section of a particular reaction was calculated for various identified γ rays arising from the same product nucleus. For this purpose only those γ rays were considered that had good statistics. The reported value is the weighted average [25] of the various cross-section values so obtained. All the decay parameters of the nuclei studied here were taken from the Table of Isotopes by Lederer and Shirley [26].

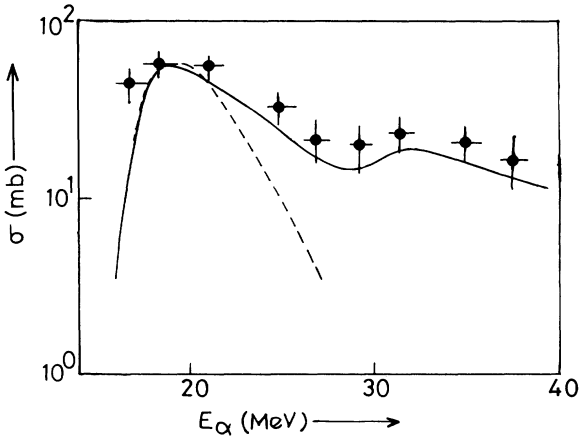

FIG. 2. Experimental and theoretical excitation functions for the reaction ^{191}Ir(α,n)^{194}Au. ●, present work; (— — —), pure EQ; and (——), EQ with the PE [$n_0=4(2n+2p+0h)$] GDH model.

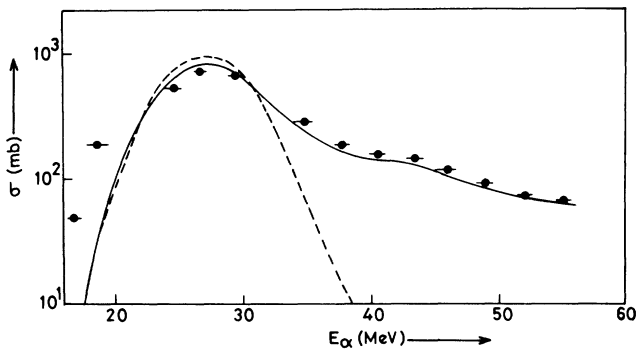

FIG. 3. Experimental and theoretical excitation functions for the reaction ^{191}Ir(α,$2n$)^{193}Au. ●, present work; (— — —), pure EQ; and (——), EQ with the PE [$n_0=4(2n+2p+0h)$] GDH model.

III. RESULTS AND DISCUSSION

A. Theoretical predictions

The theoretical excitation function calculations were done using the compound nucleus model with and without the inclusion of the PE emission of particles. For analyzing the equilibrium (EQ) part, the compound nucleus model of Weisskopf and Ewing [27] was adopted. The contribution from the PE process has been included only at the first step of evaporation. The GDH model was used for analyzing the PE part [6]. For performing these calculations, the computer code ALICE/LIVERMORE-82 [28] was used. Since the program system and the theories involved have been discussed by several authors already, we restrict ourselves here by

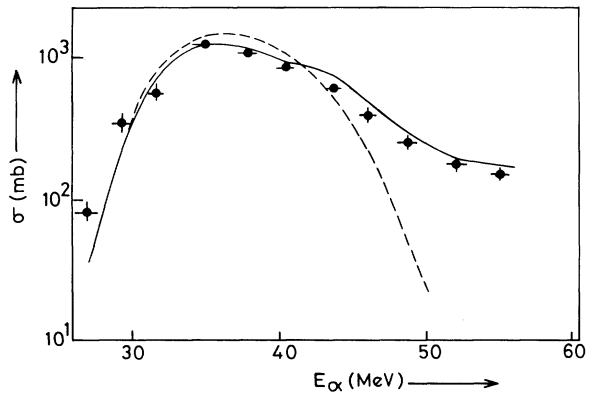

FIG. 4. Experimental and theoretical excitation functions for the reaction ^{191}Ir(α,$3n$)^{192}Au. ●, present work; (— — —), pure EQ; and (——), EQ with the PE [$n_0=4(2n+2p+0h)$] GDH model.

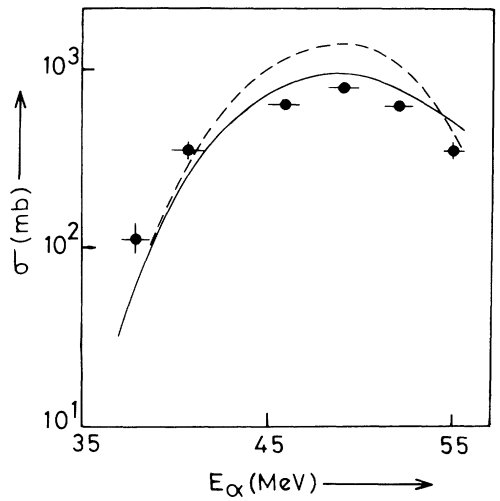

FIG. 5. Experimental and theoretical excitation functions for the reaction ^{191}Ir(α,4n)^{191}Au. ●, present work; (— — —), pure EQ; and (——), EQ with the PE [n_0=4(2n +2p +0h)] GDH model.

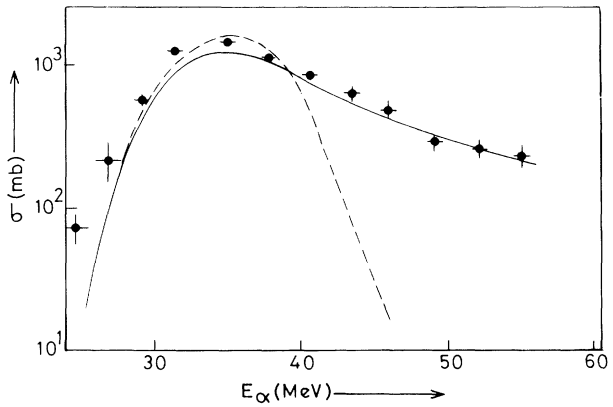

FIG. 7. Experimental and theoretical excitation functions for the reaction ^{193}Ir(α,3n)^{194}Au. ●, present work; (— — —), pure EQ; and (——), EQ with the PE [n_0=4(2n +2p +0h)] GDH model.

referring only to a review of Blann [3] on PE decay. The statistical model part of ALICE/LIVERMORE-82 can account for a large veriety of reaction types [29,30], clusters such as deuterons and α particles can be considered in addition to the evaporation of neutrons and protons according to Weisskopf and Ewing. Using a level density assuming $\rho(J) \propto 2J+1$, i.e., no constraint on angular momenta. For the level density parameter, the value of $A/8$ was taken since it is not possible in the code to use an individual level density parameter for a particular residual nucleus [30]. In the PE calculations, the initial exciton number n_0=4 with configuration (2n +2p +0h) was taken, which is the best choice for α-induced reactions [31–34].

B. Experimental results

The measured excitation functions for the reactions ^{191}Ir(α,n), ^{191}Ir(α,2n), ^{191}Ir(α,3n), ^{191}Ir(α,4n), ^{191}Ir(α,5n), ^{193}Ir(α,3n), ^{193}Ir(α,4n), and ^{193}Ir(α,5n) are shown in Figs. 2–9. Our experimentally measured results are shown by the solid circles. The total estimated energy spread is shown by the horizontal bar and the cross-sectional error is shown by the vertical bar. Where no vertical bar is shown, the error is within the data points.

In the reactions ^{191}Ir(α,n) and ^{193}Ir(α,3n); ^{191}Ir(α,2n) and ^{193}Ir(α,4n), ^{191}Ir(α,3n) and ^{193}Ir(α,5n), the product nuclei is the same, so all the decay parameters are the same but differ in Q value. As a result, the observed activity in the irradiated sample is the composite activity

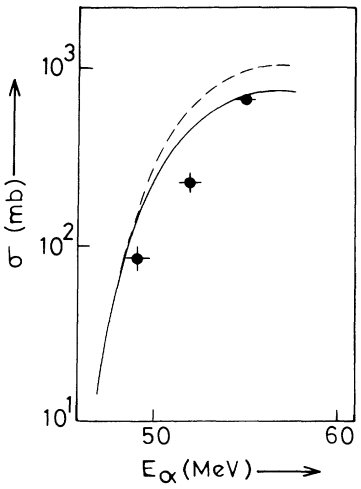

FIG. 6. Experimental and theoretical excitation functions for the reaction ^{191}Ir(α,5n)^{190}Au. ●, present work; (— — —), pure EQ; and (——), EQ with the PE [n_0=4(2n +2p +0h)] GDH model.

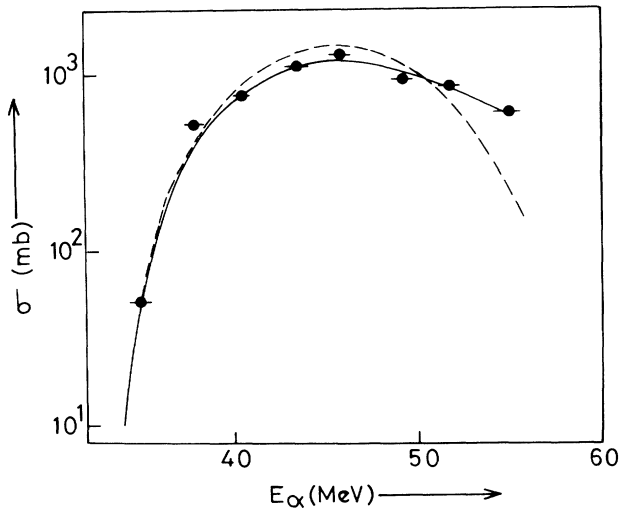

FIG. 8. Experimental and theoretical excitation functions for the reaction ^{193}Ir(α,4n)^{193}Au. ●, present work; (— — —), pure EQ; and (——), EQ with the PE [n_0=4(2n +2p +0h)] GDH model.

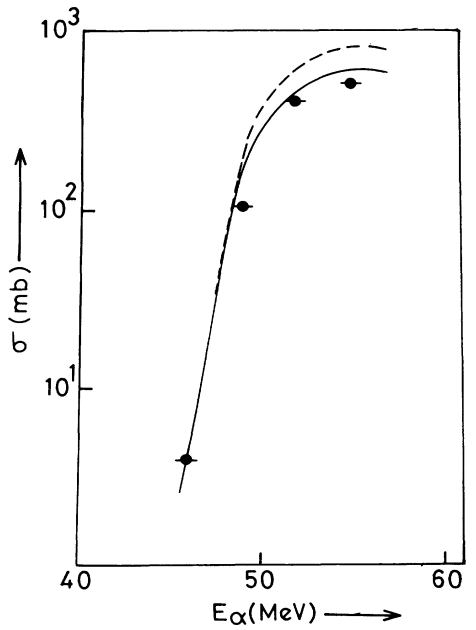

FIG. 9. Experimental and theoretical excitation functions for the reaction ^{193}Ir(α,5n)^{192}Au. ●, present work; (— — —), pure EQ; and (——), EQ with the PE [n_0=4(2n +2p +0h)] GDH model.

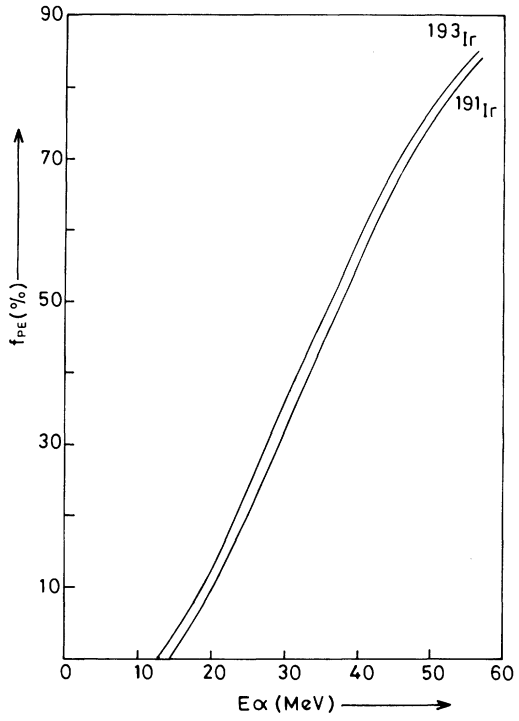

FIG. 10. Preequilibrium fraction f_{PE} of the total reaction cross section as a function of the α-particle energy.

due to the reactions in the same set mentioned above. For example, below the threshold of ^{193}Ir(α,5n), the observed activity is due to the ^{191}Ir(α,3n) reaction only, but beyond it, the observed activity will be the total of the activities produced due to these two reactions. In this overlapping region the cross sections are divided in the ratio of the theoretical cross sections of these two reactions.

In the reactions ^{191}Ir(α,n) and ^{193}Ir(α,3n), ^{191}Ir(α,2n) and ^{193}Ir(α,4n), ^{191}Ir(α,3n) and ^{193}Ir(α,5n), the product nuclei have one or more isomeric states other than the ground state. In all these cases the half-lives of the isomeric states are very short (sec/msec), so the contribution of these to the excitation function could not be measured distinguishably due to a long cooling time because the high activity was there. But, these isomeric states decay to the ground state, so the total excitation functions were measured.

Since all the measurements are reported for the first time to the best of our knowledge, that is why no literature value is shown in the figures but the presently measured results match very well with the theoretical results.

IV. CONCLUSION

The excitation functions of eight α-induced reactions have been measured for ^{191}Ir and ^{193}Ir. The experimental data and the results of geometry-dependent hybrid model calculations are in surprising agreement without any parameter adjustment for individual product. In the tail portion of the excitation functions, the experimental data and the results from the Weisskopf-Ewing model calculations are not in agreement, this is due to the PE process, which has not been considered in this model. For α-induced reactions, the choice of a four-exciton state (2n +2p +0h) for the initial configuration of the compound system gives satisfactory results and supports the finding of many earlier investigators [30–33]. The preequilibrium fraction (f_{PE}) for ^{191}Ir and ^{193}Ir has also been calculated and shown in Fig. 10. It is concluded that the preequilibrium fraction increases very fast with the increase of incident α-particle energy. The threshold for preequilibrium emission is higher for the lower mass number. It is also concluded that the value of f_{PE} is higher for the system of higher mass number at a given α-particle energy.

ACKNOWLEDGMENTS

The authors are grateful to the Department of Physics, Aligarh Muslim University, Aligarh, for providing the facilities to carry out this work and to Dr. S. N. Chintalapudi and VECC personnel for their kind cooperation during the experiment. Two of the authors (M.K.B.) and (I.A.R.) are thankful to the University Grants Commission and Council of Scientific and Industrial Research, New Delhi, for financial support.

[1] J. J. Griffin, Phys. Rev. Lett. **17**, 478 (1966).
[2] G. D. Harp and J. M. Miller, Phys. Rev. C **3**, 1847 (1971).
[3] M. Blann, Annu. Rev. Nucl. Sci. **25**, 123 (1975).
[4] E. Gadioli, E. Gadioli-Erba, and P. G. Sona, Nucl. Phys. A **217**, 589 (1973).
[5] M. Blann, Phys. Rev. Lett. **27**, 337 (1971); **27**, 700(E) (1971); **27**, 1550(E) (1971).
[6] M. Blann, Phys. Rev. Lett. **28**, 757 (1972).
[7] G. D. Harp, J. M. Miller, and J. B. Berne, Phys. Rev. **165**, 1166 (1968).
[8] C. K. Cline and M. Blann, Nucl. Phys. **A172**, 225 (1971).
[9] D. Agassi, H. A. Weidenmuller, and G. Mantzouranis, Phys. Rev. **22**, 145 (1975).
[10] T. Tamura, T. Udagawa, D. H. Feng, and K. K. Kan, Phys. Lett. **68B**, 109 (1977).
[11] T. Tamura and T. Udagawa, Phys. Lett. **78B**, 189 (1978).
[12] P. E. Hodgson, ICTP Report SMR/284-5, 1988.
[13] H. Feshbach, A. Kerman, and S. Koonin, Ann. Phys. **125**, 429 (1980).
[14] L. Avaladi, R. Bonetti, and L. Colli-Milazzo, Phys. Lett. **94B**, 463 (1980).
[15] G. M. Field, R. Bonetti, and P. E. Hodgson, J. Phys. G **12**, 93 (1986).
[16] M. Ismail and A. S. Divatia, Pramana J. Phys. **30**, 193 (1988).
[17] J. Ernst, R. Ibowski, H. Klampfl, H. Machner, T. Mayer-Kuckuk, and R. Schanz, Z. Phys. A **308**, 301 (1982).
[18] N. L. Singh, S. Agrawal, L. Chaturvedi, and J. Rama Rao, Nucl. Istrum. Methods B **24/25**, 480 (1987).
[19] I. A. Rizvi, M. K. Bhardwaj, M. Afzal Ansari, and A. K. Chaubey, Appl. Radiat. Isot. **41**, 215 (1990).
[20] I. A. Rizvi, M. K. Bhardwaj, M. Afzal Ansari, and A. K. Chaubey, Can. J. Phys. **67**, 1091 (1989).
[21] I. A. Rizvi, M. K. Bhardwaj, M. Afzal Ansari, and A. K. Chaubey, Can. J. Phys. **67**, 870 (1989).
[22] L. C. Northcliffe and R. F. Schilling, Nucl. Data Tables A **7**, 256 (1970).
[23] U. Fano, Annu. Rev. Nucl. Sci. **13**, 1 (1963).
[24] M. Afzal Ansari, R. K. Y. Singh, M. L. Sehgal, V. K. Mittal, D. K. Avasthi, and I. M. Govil, Ann. Nucl. Energy **11**, 173 (1984).
[25] S. F. Mughabghab, M. Divadeenam, and M. E. Holden, *Neutron Cross Sections* (Academic, New York, 1981), Vol. 1, Part A, p. 89.
[26] C. M. Lederer and V. S. Shirley, *Table of Isotopes*, 7th ed. (Wiley, New York, 1978).
[27] V. F. Weisskopf and D. H. Ewing, Phys. Rev. **57**, 472 (1940).
[28] M. Blann and J. Bisplinghoff, ALICE/LIVERMORE-82, Lawrence Livermore National Laboratory Report UCID 19614, 1982.
[29] R. Michel and G. Brinkmann, Nucl. Phys. **A338**, 167 (1980).
[30] R. Michel, F. Peiffer, and R. Stuck, Nucl. Phys. **A441**, 617 (1985).
[31] I. A. Rizvi, M. Afzal Ansari, R. P. Gautum, R. K. Y. Singh, and A. K. Chaubey, J. Phys. Soc. Jpn. **56**, 3135 (1987).
[32] P. Misaelides and M. Munzel, J. Inorg. Nucl. Chem. **42**, 937 (1980).
[33] G. W. A. Newton, V. J. Robinson, and E. M. Shaw, J. Inorg. Nucl. Chem. **43**, 2227 (1981).
[34] M. Blann and T. T. Komoto, Phys. Rev. C **29**, 1678 (1984).